Available online at www.sciencedirect.com

ScienceDirect

Procedia Engineering 99 (2015) 566 – 574

Procedia Engineering

www.elsevier.com/locate/procedia

"APISAT2014", 2014 Asia-Pacific International Symposium on Aerospace Technology, APISAT2014

Numerical Simulation for Changes in Aerodynamic Characteristics along the Spanwise of "Diamond back" Wing

Junkui CHEN[a,]*, Zhijun WANG[a], Juanting ZHANG[b], Lianbo ZHANG[c], Guodong WU[a]

[a]*School of Mechatronics Engineering, North University of China, Taiyuan 030051, China;*
[b]*National Key Laboratory for Electronic Measurement Technology, North University of China, Taiyuan 030051, China;*
[c]*School of Astronautics, Beijing University of Aeronautics and Astronautics, Beijing 100191, China*

Abstract

Based on the geometry shape and design parameters of the "Diamond back" wing, the changes in aerodynamic parameters along the spanwise of "Diamondback" wing at low Reynolds number are simulated by two-dimensional computational model which uses NACA6411 airfoil. The simulation results indicate that the Transition SST turbulence model have high accuracy and creditability in solving the problem of flowing around airfoil at low Reynolds number which is undemanding to stalling characteristics; The changes in aerodynamic characteristics along the spanwise of "Diamond back" wing are mainly caused by two reasons, one is the high-pressure and low-pressure region of the lower surface of anterior airfoil which are formed by the high pressure around stagnation point at the leading edge and the differential pressure between the upper and lower surface of the posterior airfoil, the other is differential pressure change of posterior airfoil caused by air blocking; When the vertical height difference of the anterior and posterior wing is 0, these effects are mainly reflected on the part of the leading edge distance between the anterior and posterior wing that is less than 350mm; When the value is greater than 350mm, aerodynamic performance achieves optimal and aerodynamic parameters keep almost unchanged.

Peer-review under responsibility of Chinese Society of Aeronautics and Astronautics (CSAA)

Keywords: "Diamond back" wing; turbulence model; aerodynamic characteristics; changes along the spanwise; numerical simulation;

* Corresponding author. Tel.: +86-18334788826.
E-mail address: chenjk-0803@163.com

Peer-review under responsibility of Chinese Society of Aeronautics and Astronautics (CSAA)
doi:10.1016/j.proeng.2014.12.572

1. Introduction

In the past decades, the research about small UAV have become a focus in many countries because of its flexibility, simplification and portability. It has been applied to reconnaissance, communication relay link, ship bait, biochemical or nuclear material detection, etc. The remote-controlled and self-controlled UAVs are both extremely suitable for these special tasks [1]. However, there are some disadvantages on small UAV such as low speed, long time for entering the mission area and short voyage. If these disadvantages are overcome, the small UAV will play more and more important role. Therefore the combination of UAV and rocket is considered. The UAV is launched over the target region by a rocket and then starts to work. Due to the rocket flight faster than small UAV, the time for reaching the mission region and obtaining intelligence will be greatly reduced. Both the kylite MAV of Israel and the KZO of Germany for surveillance and reconnaissance are based on the concept described above.

In order to put the small UAV into the rocket launcher and improve portability, the corresponding deformation of wing is required, so the problem of wing deformation mode must be solved at first. Synthesize the aerodynamic characteristics, structural strength, complexity and reliability, the folded pattern with the "Diamond back" aerodynamic configuration was chosen finally in this study. It has many advantages such as simple and reliable folded-expanded mechanism, compact folded state, small space occupation, high lift-drag ratio, strong glide range-extended capability. Besides, it can improve the strength and stiffness of high aspect ratio folded wing and increase the critical flutter speed [2]. At present, the experiments and numerical simulations for the aerodynamic characteristics of whole "Diamond back" wing have been done, and they are mainly based on the special wing with glide range-extended capability which is installed on the high-speed loitering munition or guided bomb. The research of Lei Juanmian, Wu Xiaosheng and others show that [3,4,5,6], "Diamond back" wing has high lift, with high drag parameter, too. Overall, lift-drag ratio is relatively high; The lift and lift-drag ratio of "Diamond back" wing which has the configuration of higher anterior wing strip and lower posterior wing strip are larger than the contrary; The roll damping moment coefficient of "Diamond back" wing is greater; The aircraft with "Diamond back" wing is not suitable to fly under high angle of attack.

Because of low speed and small scale, the flight Reynolds number of small aircraft is very low (1.5×10^4~5×10^5), viscosity effect and unsteady effect are remarkable, the flow structure and aerodynamic characteristics of fixed-wing are significantly different from those at high Reynolds number [7]. If "Diamond back" wing is utilized to small UAV, the impact of low Reynolds number must be considered. Meanwhile, as a result of the outstanding spanwise flow characteristics of "Diamond back" aerodynamic configuration and the complex aerodynamic interference between the anterior and posterior wing, the aerodynamic characteristics change with the different distance from anterior to posterior wing. Therefore, the numerical simulation about these changes along spanwise at low Reynolds number has been done by FLUENT in this paper, it is based on the existing research of high-speed and whole aerodynamic characteristics, and the airfoils of the anterior and posterior wing on different spanwise position are used as the simulation models. The aim of this research is to provide reference for designing small UAV with the "Diamond back" wing.

2. "Diamond back" Wing Physical and Computational Model

2.1. Physical Model

The planary form and geometry parameters of "Diamond back" wing are shown in Fig.1, where L is the distance between the joint of anterior and posterior wing on the left and on the right, b is the distance between the leading edge of anterior and posterior wing root chord, d is the distance between the leading edges of anterior and posterior wing tip chord, x is the distance from any leading edge of anterior wing to the leading edge of the corresponding posterior wing ($d\leq x\leq b$), φ_1 is the sweep angle of anterior wing, φ_2 is the forward-swept angle of posterior wing, C_1 and C_2 are effective chord length of the anterior and posterior wing, respectively. Variable C_0 is the vertical distance between the leading edge and the trailing edge of anterior wing (Considering the configuration after folding, C_0 is also the vertical distance from the leading edge to the trailing edge of posterior wing). In addition, the vertical height difference of anterior and posterior wing ΔH is defined as the vertical distance between the lowest point on the lower surface of anterior wing and the highest point on the upper surface of the posterior wing.

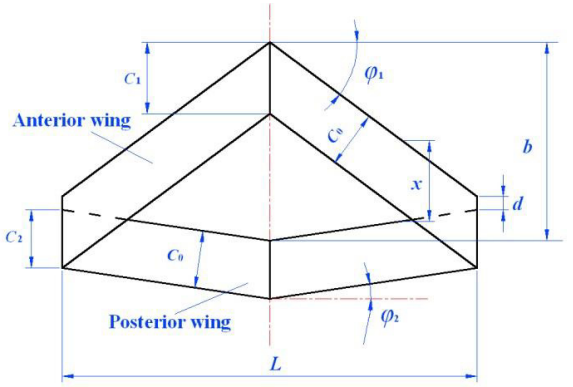

Fig. 1. Planary form and geometry parameters of the "Diamond back" wing

b, d and C_0 are determined firstly on overall design, the relationships of the other parameters varied with φ_1 and φ_2 are:

$$C_1 = C_0 / \cos\varphi_1 \tag{1}$$

$$C_2 = C_0 / \cos\varphi_2 \tag{2}$$

$$L = \frac{2(b-d)}{\tan\varphi_1 + \tan\varphi_2} \tag{3}$$

It is worth noting that the spanwise length of "Diamond back" wing is related to L, but it is not represented by L, its value is determined by the particular design of the wingtip.

2.2. Calculation Model

In order to study the characteristics and reasons of aerodynamic parameters change along the spanwise of "Diamond back" wing, the chosen simulation model was NACA6411 which had good aerodynamic properties at low Reynolds number. The geometry parameters of "Diamond back" wing were taken as C_0=130mm, φ_1=37°, φ_2 =11°, b=450mm, d=0mm, ΔH =0mm, according to Eq.(1)~Eq.(3), C_1=162mm, C_2=132mm, L=950mm. Based on C_1, C_2 and the distance changes with the leading edge of anterior and posterior wing, the values of x were taken as 0mm, 15mm, 30mm, 50mm, 100mm, 150mm, 162mm, 200mm, 250mm, 350mm, 450mm, respectively. The unit of x was millimeter and would no longer be written in the following description.

The simulated cases were using Gambit software to build the calculated model and generate C type structured grid in this paper. The computational domain boundaries were set as 25 C_1 on the up and down direction of airfoil and the upstream of flow, and 25 C_1 for x≤150 or 28 C_1 for x≥162 on the downstream of flow. The distance in normal direction of the first layer of the grid from the ground was 3.7×10^{-5}~4.3×10^{-5} C_1, which could satisfy y^+<1. The number of grid should be minimized under the premise of ensuring the calculation accuracy. Fig.2 shows the computational grid of the airfoils of "Diamond back" wing and the partial grid around the wall for ΔH =0 and x=250.

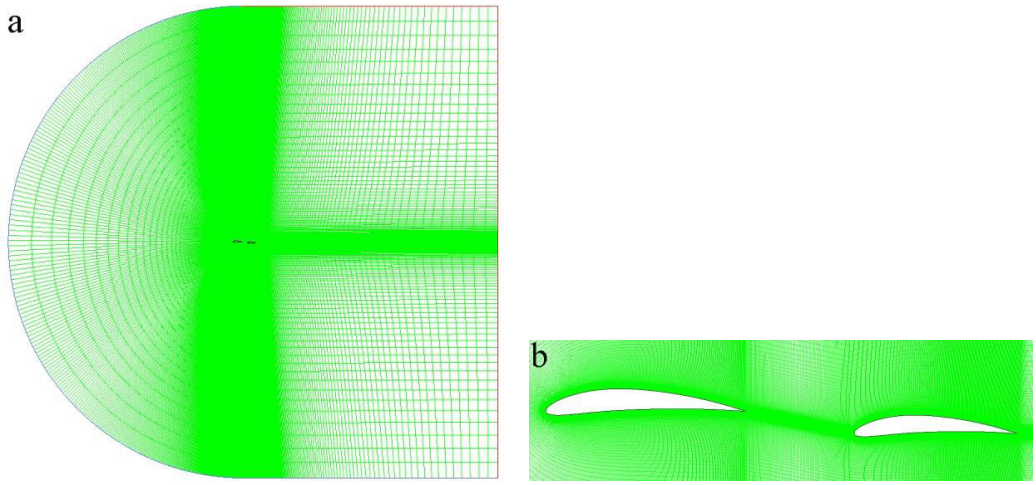

Fig. 2. Computational grid of the airfoils of "Diamond back" wing for ΔH =0 and x=250. (a) C type structured grid; (b) Partial grid around the wall

3. Numerical Methods

3.1. Calculation Method

Fluent software was used to calculate in this paper, the flow was set as steady and incompressible, governing equations were the mass-weighted N-S equations which is discretized by Finite Volume Method and solved by SIMPLE method. The convection term was discretized by second order upwind scheme while the diffusion term was discretized by central difference scheme. The boundary conditions were Velocity-Inlet and Pressure-Outlet, and the flow velocity and angle of attack of inlet were set to 34m/s and 4° respectively, then the Reynolds number was about 3.5×10^5 based on the chord length of 162mm.

3.2. Turbulence Model

In this paper, the four-equation Transition SST model was employed. It was based on the coupling of the appropriate correction SST *k-ω* turbulence model with the γ-$\mathrm{Re}_{\theta t}$ transition model developed by Langtry and Menter [8,9,10]. This model combines the advantages of the transition empirical relationships and low Reynolds number turbulence model, so it not only can reflect some transition mechanism, but also is suit for engineering calculation [11].

Specific expressions and related constants of Transition SST model are detailed in reference [12].

4. Results and Analysis

4.1. Numerical Method Validation

In order to verify the accuracy and credibility of numerical method, the E387(E) airfoil was chosen to simulate, and the numerical results were compared to the experiments performed in the low-turbulence wind tunnel in the Subsonic Aerodynamics Research Laboratory at the University of Illinois at Urbana-Champaign (UIUC) [13,14]. E387 airfoil was designed for glider by Richard Eppler in the early 1960s, and it was a typical high-lift airfoil under low Reynolds number. In recent years, E387 was often used to compare with other low Reynolds number airfoils in the wind tunnel experiments as a benchmark airfoil.

In this numerical simulation, the inlet velocity was set to 20.25m/s, angles of attack were varied from -6° to 12°

in 2° increment, Reynolds number was 3.0×10^5 based on the chord length, Spalart-Allmaras turbulence model, SST *k-ω* turbulence model and Transition SST model were employed, respectively. Then the numerical results and experimental data about lift and drag coefficients were shown in Fig.3.

As can be seen from Fig.3(a), when the angles of attack are -6°, 10° and 12°, the lift coefficients calculated by Spalart-Allmaras turbulence model have relatively high error, its values are 20.2%, 8.5% and 11.95%, respectively. While the values calculated by SST *k-ω* turbulence model and Transition SST model show excellent agreement with experimental data, except for the maximum error which is 3.4% between 10° and 12°.

As can be seen from Fig.3(b), the drag coefficients calculated by Transition SST model are more coincident with experimental data than Spalart-Allmaras turbulence model and SST *k-ω* turbulence model. It is more obvious with the angles of attack from 0° to 12°. Compared drag coefficients calculated by Transition SST model with the experiments, the error is about 26% near 12°, while the others are well agree with experimental data, and the whole changing trend is identical.

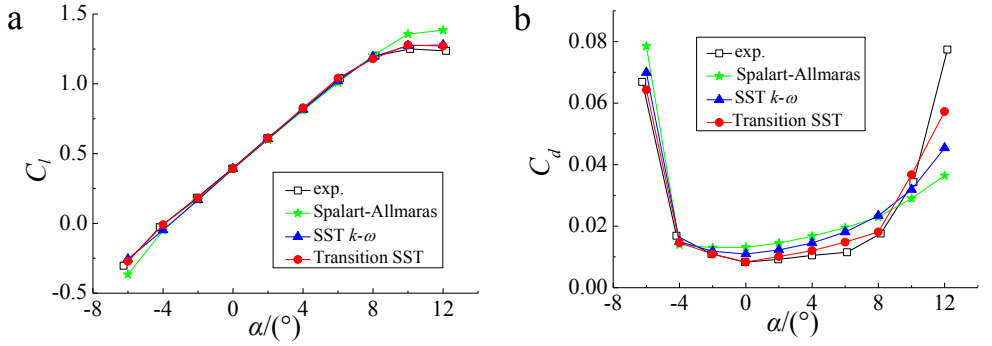

Fig. 3. Comparison of numerical and experimental values of E387(E) airfoil. (a) Lift coefficients; (b) Drag coefficients.

It can be seen that the results obtained by Transition SST model are closer to the experimental data than SST *k-ω* model and Spalart-Allmaras model from -6° to 10°, and the credibility is relatively high. It is worth noting that the flow separation occurs early at the trailing edge and will not reattach in the stall condition, as shown in Fig.4. The turbulence is in a strong non-equilibrium state after separation, while the SST *k-ω* turbulence model is based on simple boundary equilibrium turbulence, so it can not accurately predict the non-equilibrium transport properties of turbulence, which leads to the poor effect for simulating the stalling characteristics of flowing around airfoil [15]. In addition, when the flow is in the stalling state, the transition is not the key factor in inaccurate simulation for airfoil aerodynamic characteristics [16,17]. Therefore, the simulation results have great error near the stall angle(12°) in Transition SST model.

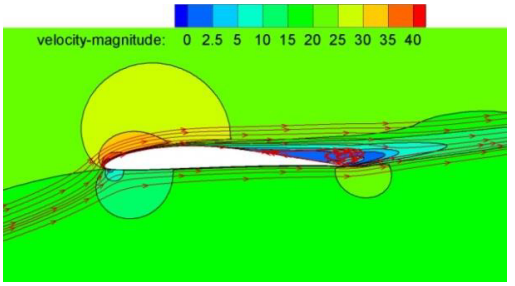

Fig. 4. Velocity contour and streamlines for Transition SST model at the angle of attack of 12°

Thus, based on the method above and by employing Transition SST model to solve the problem of flowing around airfoil at low Reynolds number which is undemanding to stalling characteristics, the simulated results show higher accuracy and credibility than Spalart-Allmaras turbulence model and SST *k-ω* turbulence model, and can

satisfy the requirements of engineering studies.

4.2. Results Analysis

When ΔH =0, the curves of lift coefficient, drag coefficient and lift-drag ratio vary with x are shown in Fig.5. The data of x=0 should be noted, and its velocity contour and streamlines are shown in Fig.6. Due to the air blocking caused by the anterior wing, the flow occur large separation very early at the trailing edge of the posterior wing and will not reattach, this phenomenon is similar to flow state in the stalling. Based on the analysis described above, it can be seen that the lift coefficient is larger than the experiments, however the drag coefficient is smaller than the experiments, so the data of x=0 are abnormal in the whole changing trend. Taking into account the large error, these data at this point are no longer used in the subsequent analysis.

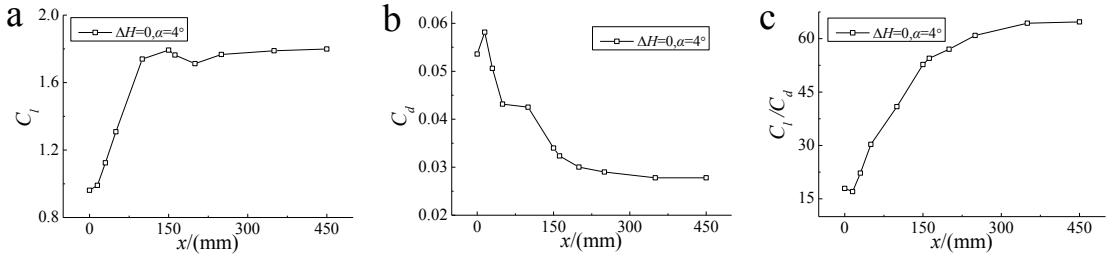

Fig. 5. Change trend of aerodynamic parameters vary with x for ΔH =0. (a) Lift coefficients; (b) Drag coefficients; (c) Lift-drag ratios.

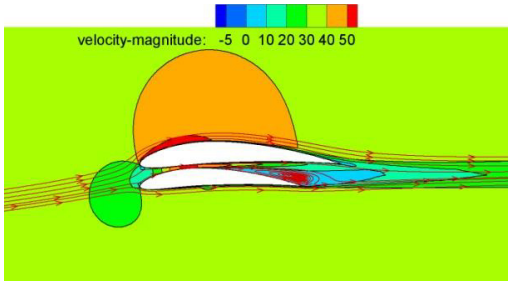

Fig. 6. Velocity contour and streamlines for x=0

4.2.1 Aerodynamic Characteristics Analysis for Lift Coefficients Vary with x

Fig.7 illustrate the pressure contour of NACA6411 single-airfoil with 162mm chord length at α=4° and the pressure contours of anterior and posterior airfoils at different x. Compared with the single-wing configuration, the high-pressure and low-pressure region are formed on the lower surface of anterior airfoil which due to the high pressure region near the stagnation point at the leading edge of posterior airfoil and the differential pressure between the upper and lower surface caused by the flowing around airfoil. Meanwhile, influenced by the air blocking of anterior wing to posterior wing, the effective angle of attack of posterior airfoil is smaller than the free-stream, then the differential pressure distribution between the upper and lower surface is different from the single-wing.

As can be seen from the figures, the ranges of high-pressure region move backward and increase gradually with increasing x, meanwhile the ranges of low-pressure region move backward and decrease gradually, so the lifts increase gradually. Fig.7(d) shows that when x=150, the range of high-pressure region on the lower surface of anterior wing reaches maximum, while the low-pressure region of posterior wing no longer influences on the anterior wing, thus the whole lift of double wings achieves maximum. When $150 < x \le 200$, the influence of high-pressure regions to the anterior wing are decreasing, that is to say the pressures on the lower surface of anterior wing decrease gradually, while the air blocking caused by anterior wing to posterior wing has not disappeared, so the whole lifts have slight decline; when x>200, the influence of high-pressure region to the anterior wing weaken to

minimum, at the same time, the influence of air blocking to the posterior wing decrease rapidly, that is the differential pressures between the upper and lower surface increase, thus these combined effects make the whole lifts gradually stabilized after the rebound.

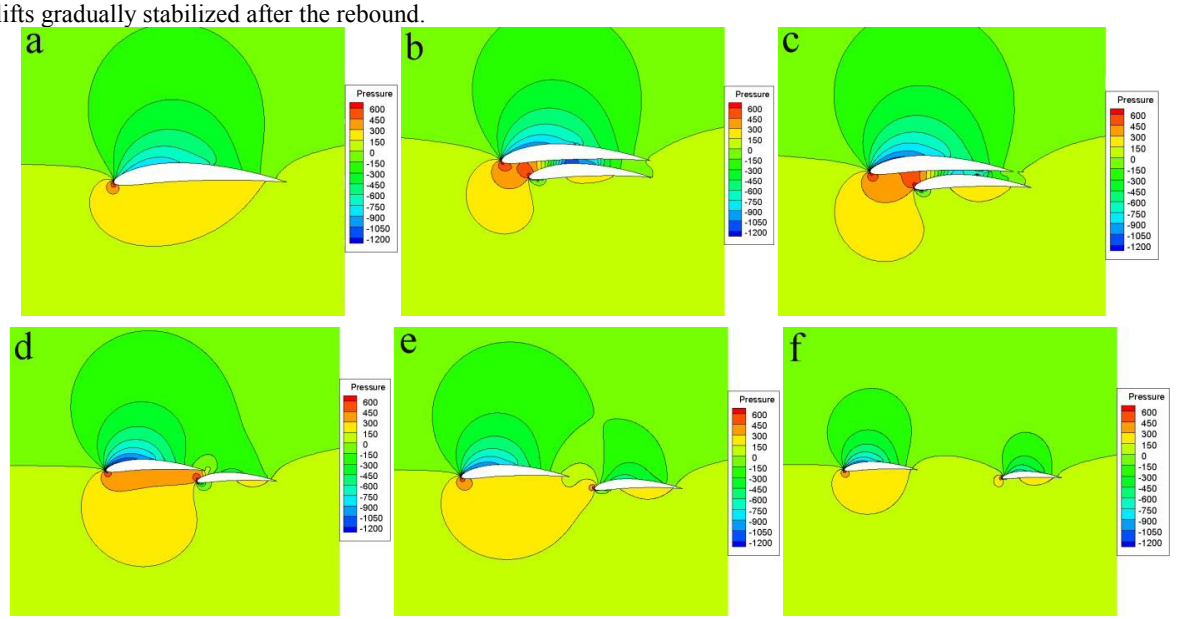

Fig. 7. Comparison of Pressure contour of the single-airfoil and the anterior&posterior airfoils at different x. (a) Single-airfoil; (b) x=30; (c) x=50; (d) x=150; (e) x=200; (f) x=350

4.2.2 Aerodynamic Characteristics Analysis for Drag Coefficients Vary with x

Fig.8 show the pressure coefficient distribution of NACA6411 single-airfoil with 162mm chord length at α=4° and the pressure coefficient distributions of anterior and posterior airfoils at different x. When x=15, the pre and post differential pressure distributions on the upper surface of anterior wing and the lower surface of posterior wing are similar to the single-wing, but affected by high-pressure and low-pressure region, the pressure distributions on the lower surface of anterior wing and the upper surface of posterior wing decrease first and then increase along the chordwise, which makes pressure drag increase greatly than single-wing, thereby the whole drag reaches maximum at this position. With the increasing of x, the ranges of high-pressure region on the lower surface of anterior wing increase and the ranges of the low-pressure region gradually move backward until disappearance, meanwhile the values of the low-pressure region on the upper surface of posterior wing increase gradually, thus the whole drags decrease continuously due to the combined effect. When x=200, the low-pressure region on the lower surface of anterior wing is almost disappeared, two main factors which affect the drag change have reduced to one, thus the decreased magnitude of the drag coefficient decreases with the increasing of x. When x=350, the interaction between anterior and posterior wing has been relatively small, this lead to the pressure distributions on the upper and lower surface of anterior and posterior wing are similar to the single-wing respectively, so the whole drags keep almost unchanged during $350 < x \le 450$.

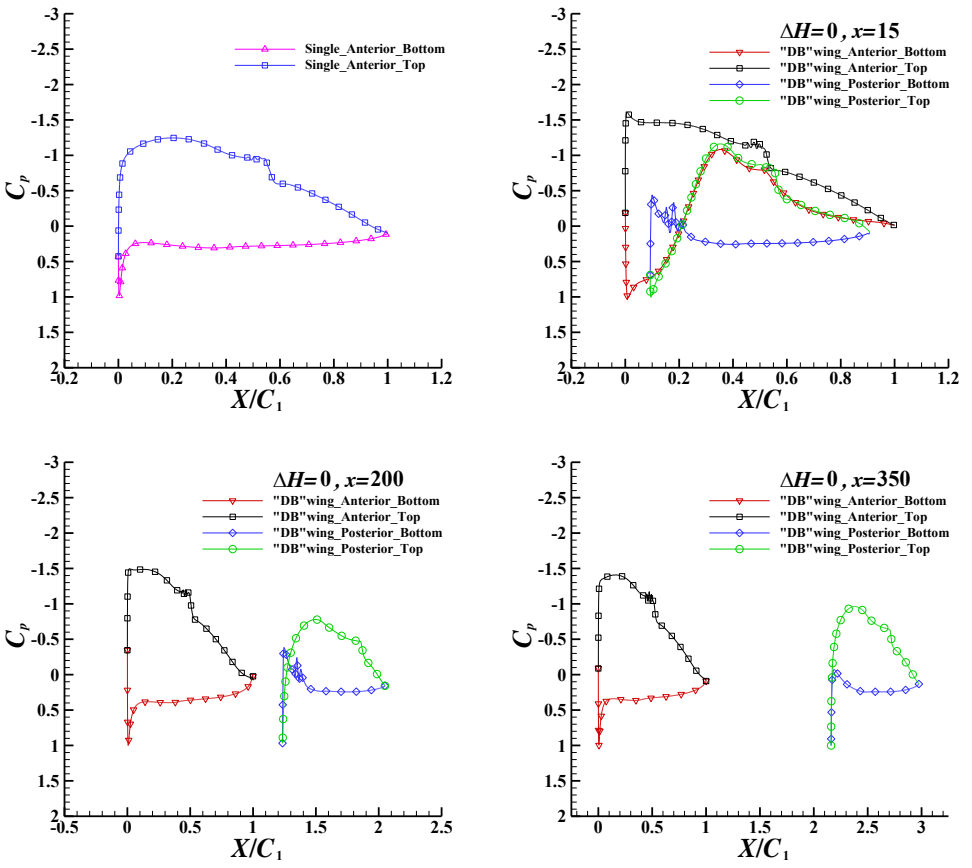

Fig. 8. Comparison of C_p distributions of the single-airfoil and the anterior&posterior airfoils at different x

4.2.3 Aerodynamic Characteristics Analysis for Lift-drag Ratio Vary with x

As can be seen from Fig.5(c), owing to the change of lift coefficients and drag coefficients, lift-drag ratios increase continuously and the increased amplitude decrease gradually during $15 \le x \le 350$; Lift-drag ratios increase slightly and then tend to steady during $350 < x \le 450$.

Through the above analysis it can be seen that the reasons why lift coefficients and drag coefficients of "Diamond back" wing are respectively different at different x is that there is an interaction between the anterior and posterior wing. That is to say the aerodynamic characteristics vary along the spanwise of "Diamond back" wing are mainly caused by two reasons, one is the change of high-pressure and low-pressure region on the lower surface of anterior airfoil, the other is the decrease of effective angle of attack on the posterior wing owing to the air blocking of anterior wing to posterior wing. Meanwhile, it can be seen from Fig.5, these interactions are mainly reflected at $0 \le x \le 350$, when $x > 350$, the lift coefficients, drag coefficients and lift-drag ratios keep almost unchanged with the increasing of x.

5. Conclusion

(1) If the stalling characteristics is undemanding in solving the problem of flowing around airfoil at low Reynolds number though the method of numerical simulation, the flow can be set as steady and incompressible, meanwhile the boundary conditions use Velocity-Inlet and Pressure-Outlet, and the turbulence model employs Transition SST

model, then the simulation results will have high accuracy and creditability, and can be used for engineering studies.

(2) The changes in aerodynamic characteristics along the spanwise of "Diamond back" wing are mainly caused by two reasons, one is the high-pressure and low-pressure region on the lower surface of anterior airfoil, which are formed by the high pressure around stagnation point at the leading edge and the differential pressure between the upper and lower surface of the posterior airfoil; the other is the decrease of effective angle of attack on the posterior wing and the change of differential pressure between the upper and lower surface of posterior airfoil, which are caused by the air blocking of anterior wing to posterior wing.

(3) When the vertical height difference of anterior and posterior wing is 0mm, these effects are mainly reflected on the part of $0 \le x \le 350$, when $x > 350$, the aerodynamic performances achieve optimal and the aerodynamic parameters keep almost unchanged with the increasing of x.

(4) According to the overall design and the actual project requirement, the leading edge distance between the tip chord of the anterior and posterior wing should be designed rationally to use effectively the positive influence of the high pressure around stagnation point at the leading edge of posterior airfoil, reduce the negative influence of the air blocking, and decrease the proportion of unfavorable aerodynamic performance, meanwhile, it is one of the effective optimization methods for "Diamond back" aerodynamic configuration.

References

[1] Mueller, TJ & Delaurier, JD 2003, 'Aerodynamics of Small Vehicles', *Annual Review of Fluid Mechanics*, vol. 35, pp. 89-111.
[2] Lei, JM, Hu, J & Wu, JS 2004, 'Aerodynamic problems of small diameter bomb', *Journal of Projectiles, Rockets, Missiles and Guidance*, vol. 24, no. 3, pp. 169-170.
[3] Lei, JM, & Wu, JS 2006, 'Effect of diamond backwing geometric parameters to the aerodynamic characteristics', *Transactions of Beijing Institute of Technology*, vol. 26, no. 11, pp. 945-948.
[4] Lei, JM, & Wu, JS 2007, 'Wind Tunnel Experiment for Aerodynamic Characteristics of Diamond Back Wings', *Acta Armamentarii*, vol. 28, no. 7, pp. 893-896.
[5] Wu, XS, Lei, JM & Wu, JS 2010, 'Numerical Simulation for Aerodynamic Characteristics of Diamond back Wing', *Acta Armamentarii*, vol. 31, no. 8, pp. 1048-1052.
[6] Wu, XS 2010, 'Investigation into Aerodynamic Characteristics of Folding Wing Guided Bomb', *Transactions of Beijing Institute of Technology*, vol. 30, no. 9, pp. 1024-1027.
[7] Li, F, Bai, P, Shi, W & Li, JW 2007, 'Low Reynolds Number Aerodynamics of Micro Air Vehicles', *Advances in Mechanics*, vol. 37, no. 2, pp. 257-268.
[8] Langtry, RB, & Menter, FR 2005, 'Transition modeling for general CFD applications in aeronautics', AIAA2005-0522.
[9] Menter, FR, Langtry, RB, Likki, SR, et a1. 2004, 'Acorrelation-based transition model using local variables part I-Model formulation', GT2004-53452.
[10] Menter, FR, Langtry, RB, Likki, SR, et a1. 2004, 'Acorrelation-based transition model using local variables part II-Test cases and industrial applications', GT2004-53454.
[11] Liu, PQ, Ma, LC, Qu, QL & Duan, ZZ 2013, 'Numerical investigation of the laminar separation bubble control by blowing/suction on an airfoil at low Re number', *Acta Aerodynamic Sinica*, vol. 31, no. 4, pp. 518-524 (540).
[12] *ANSYS 14.0 FLUENT Theory Guides* 2011, ANSYS, Inc.
[13] Selig, MS, Deters, RW & Williamson, GA 2011, 'Wind tunnel testing airfoil sat Low Reynolds Numbers', AIAA2011-875.
[14] Selig, MS, & McGranahan, BD 2004, 'Wind Tunnel Aerodynamic Tests of Six Airfoils for Use on Small Wind Turbines', *Journal of Solar Energy Engineering*, vol. 126, no. 4, pp. 986-1001.
[15] Wen, XQ, Liu, YW, Fang, L & Lu, LP 2013, 'Improving the capability of k-ω SST turbulence model for predicting stall characteristics of airfoil', *Journal of Beijing University of Aeronautics and Astronautics*, vol. 39, no. 8, pp. 1127-1132.
[16] Langtry, RB, Gola, J & Mente, FR 2006, 'Predicting 2D airfoil and 3Dwind turbine rotor performance using a transition model for general CFD codes', AIAA2006-395.
[17] Shelton, A, Abras, J, Jurenko R, et al. 2005, ' Improving the CFD predictions of airfoils install', AIAA2005-1227.